

# RADIATION EFFECTS ON SATURN'S ICY MOON ENCELADUS

M. J. Loeffler, U. Raut and R. A. Baragiola

*University of Virginia, Laboratory for Atomic and Surface Physics, Engineering Physics,*

*Charlottesville, VA 22904, USA*

## Abstract

Recently the Cassini spacecraft observed unexpected emission of plumes of water vapor and ice particles from the southern polar region of Enceladus. Here we show that similar behavior appears when heating water-ammonia ices that have been irradiated with energetic ions typical of Saturn's magnetosphere. In addition, we also show the rapid decrease in the ammonia infrared absorptions during ion irradiation. Finally, we observed the thermal release of nitrogen that may explain the intriguing finding of  $N^+$  in the inner magnetosphere and  $N_2$  in the plume emitted from Enceladus.

The measurements of Voyager, remote sensing, and more recently the Cassini spacecraft have shown unique conditions at and around Enceladus. The surface of this satellite is the brightest (1) and most diverse among the Saturnian satellites (2). Furthermore, the densest part of the E-ring (2) and a neutral OH torus (3) fall near the orbit of Enceladus suggesting that they originate from sources in this satellite. Besides water and its dissociation products, Cassini detected nitrogen from an unknown source near Enceladus (4, 5). Recent flybys have shown temperatures as high as 145 K near the South Pole (6), much higher than the average surface temperature [ $\sim 51$  K] (7). In addition, Cassini detected a spectacular fountain of water ice particles and vapor emanating from this south-polar region (8, 9). This is astounding since, even at 145 K, water evaporates at a rate (10) that is many orders of magnitude slower than needed to entrain particles observed in this fountain.

The origin of the varied terrain, thermal anomalies, water bursts, nitrogen in the inner magnetosphere, E-ring particles and OH Torus remains largely unexplained. Since the first measurements of Voyager, it has been thought that Enceladus is geologically active (2, 11), possibly due to tidal heating (12) which could be enhanced by an orbital resonance (13). Such a heat source could melt a subsurface material, such as a solid solution of water and ammonia (14, 15), which has an eutectic point of 173 K at the dihydrate composition  $[NH_3 \cdot 2H_2O]$ . The liquid could surface occasionally when cracks open, producing new smooth terrain, or burst out in cryovolcanism (12), which could feed the E-ring. Since Enceladus is embedded in Saturn's magnetosphere, ion irradiation

may preferentially remove ammonia by sputtering (16) which would allow a much lower  $NH_3$  concentration on the surface (17) than in the bulk. The effects of magnetospheric ion irradiation are evident in the chemical alteration of the surfaces of satellites of Jupiter (18) and other satellites of Saturn (19).

Here, we present laboratory studies of ion irradiation and thermal annealing of water-ammonia mixtures. The experiments were performed in vacuum at  $2 \times 10^{-10}$  Torr using a mass-analyzed beam of 100 keV protons, typical of Saturn's magnetosphere (20). Solid ammonia-water films were grown at 80 K on the gold mirror surface of a quartz-crystal microbalance (QCM) to a thickness of  $\sim 2 \mu m$  [ $148 \mu g/cm^2$ ], slightly larger than the depth of penetration of the ions (21). The mixtures were grown using two separate gas dosers with the 1:2  $NH_3:H_2O$  ratio of the dihydrate, as this is one of the equilibrium phases for ice mixtures with  $< 65.4$  wt% ammonia (22). The samples were then annealed to 120 K to achieve uniform mixing. Irradiations were done at 70 K while monitoring the samples with infrared reflectance (1.5-15  $\mu m$ ), a mass spectrometer (MS) aimed at the surface, and gravimetry using the microbalance. More experimental details can be found in Ref. 23.

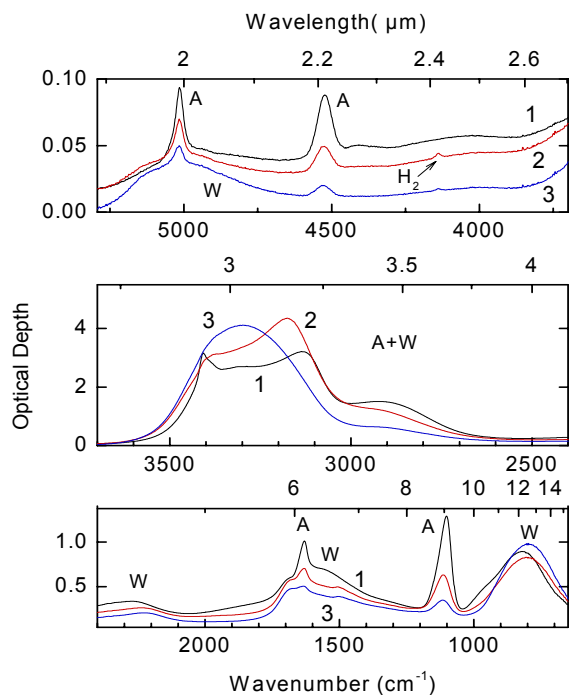


Figure 1. 1:2 ammonia-water mixture at 70 K before (1) and after irradiation with  $2.45 \times 10^{15} \text{ H}^+/\text{cm}^2$  (2) and  $9.5 \times 10^{15} \text{ H}^+/\text{cm}^2$  (3) at 100 keV. Features are labeled as W for water and A for ammonia.

Fig. 1 shows the evolution of the infrared spectra of an ice mixture during irradiation. The spectra are dominated by water and ammonia features, but small bands emerge at  $4139 \text{ cm}^{-1}$  from  $\text{H}_2$  and at  $2325 \text{ cm}^{-1}$  from  $\text{N}_2$ . These dipole transitions in  $\text{H}_2$  and  $\text{N}_2$  are forbidden for the free molecules; their appearance is likely due to symmetry breaking perturbations at defect sites [e.g., molecules trapped at vacancies]. The fluence dependence of the band areas of infrared transitions for  $\text{NH}_3$  [ $4523 \text{ cm}^{-1}$ ],  $\text{H}_2$ , and  $\text{N}_2$  are shown in Fig. 2 [top]. The mass loss measured by the microbalance during the course of this experiment shows that  $<30\%$  of the ammonia is removed by ion impact [sputtering]. Thus, the 81% drop in the  $\text{NH}_3$  band area is due to the decomposition of the molecule and formation of radiation products trapped in the ice, that include  $\text{H}_2$  and  $\text{N}_2$  [Fig. 2 top]. The two lower panels in Fig. 2 show the fluxes of ejected  $\text{H}_2$  and  $\text{N}_2$  measured by the MS, and the total sputtering yield, defined as the number of molecules ejected per incident ion. These quantities increase with fluence peaking at  $\sim 2\text{-}3 \times 10^{15} \text{ ions/cm}^2$  suggesting that they are related to the accumulation of trapped species, such as H,  $\text{H}_2$ , N,  $\text{NH}_x$  and  $\text{N}_2$ . Although the MS signal due to the  $\text{NH}_3$  is masked by OH from the water background, we could monitor the NH cracking product with the MS and found it to be below the noise level during irradiation,

indicating that ejection of intact  $\text{NH}_3$  molecules is at most a minor contributor to sputtering. The drop in the sputtering yield and the MS signals at high fluences is correlated with the depletion of the radiolytic products [and ammonia] inside the film. We note that these processes do not have a thermal origin, since interruption of irradiation stopped changes in the infrared spectra, the outgassing flux and the mass loss.

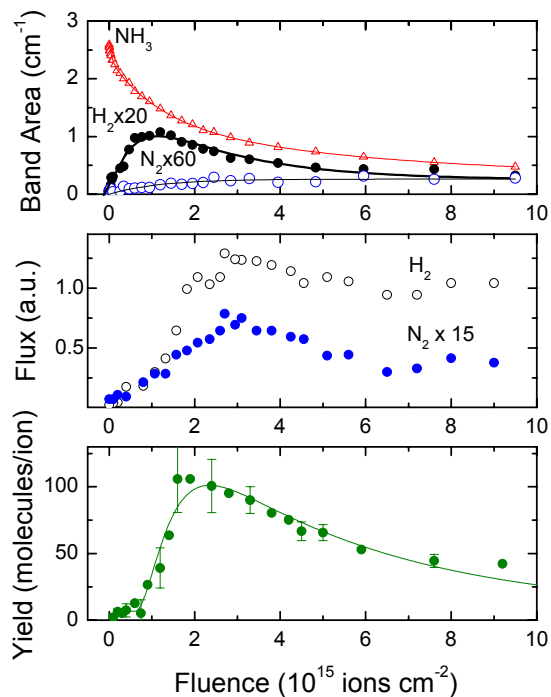


Figure 2. Evolution of a 1:2 ammonia-water mixture during irradiation with 100 keV protons at 70 K. Top: Fluence dependence of the infrared band area of  $\text{NH}_3$ ,  $\text{H}_2$ , and  $\text{N}_2$ . Middle: Gas ejection measured by the mass spectrometer. Bottom: Sputtering yield averaged over different experiments. The sputtering yield was calculated by dividing the mass loss by 17 amu. The lines shown are to guide the eye.

To explore the effects of temperature changes on the irradiated ices, we warmed the samples [0.2 K/min] after irradiation, while measuring the infrared spectra, the mass loss and the flux of the desorbed gas [Fig. 3]. The  $\text{H}_2$  and  $\text{N}_2$  band areas decrease steadily during warming, even though there are no corresponding changes in the QCM and MS between 70 and 115 K. Since this decrease in the band area is not due to a loss of molecules it is likely related to the

annealing of defects that enabled these dipole forbidden transitions, as has been seen for O<sub>2</sub> in condensed gases (24).

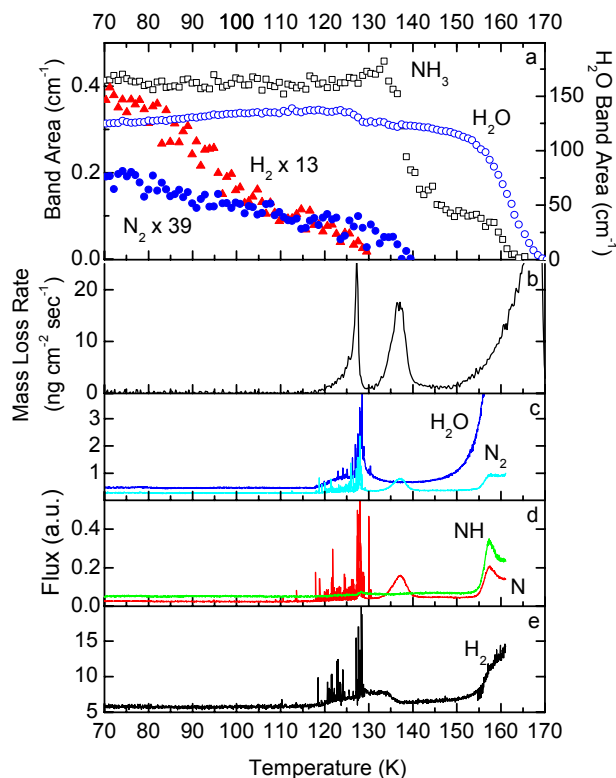


Figure 3. Evolution of a 1:2 ammonia-water sample irradiated with  $7.5 \times 10^{15} \text{ H}^+/\text{cm}^2$  at 70 K during warming at 0.2 K/min. a) Band areas calculated from the infrared spectra, b) Mass loss rate from microbalance ( $\text{ng cm}^{-2} \text{ sec}^{-1}$ ), and c-e) Desorbed flux from the MS. The MS data is not plotted beyond 161 K because it includes molecules coming from surfaces outside the irradiated area.

During warming we observed two types of gas ejection: the usual thermal outgassing and striking fast bursts [ $\sim 0.5$  second in duration] occurring at a frequency that peaks at  $\sim 125\text{K}$  and ceases by  $\sim 130$  K. The mass loss from the sample during each burst was below our level of detection [ $\sim 3$  ng], but there was a cumulative loss of  $14.2 \mu\text{g}/\text{cm}^2$  due to these bursts and the underlying broad desorption peak. The bursts observed in the total flux, as is seen in the flickering of the ionization gauge, and in MS signals due to hydrogen, nitrogen and water. The broad desorption peak contains mainly water and H<sub>2</sub> with little nitrogen; we note that this desorption peak corresponds to a drop in the area of the water absorption band at  $\sim 800 \text{ cm}^{-1}$

[Fig. 3], which decreases by  $\sim 8\%$  [a loss of  $\sim 7.5 \mu\text{g}/\text{cm}^2$ ]. The next peak in the mass loss rate, at 137 K, is correlated with the emission of nitrogen, and contains  $22.1 \mu\text{g}/\text{cm}^2$  or 51% of the mass of nitrogen [in NH<sub>3</sub>] in the film before irradiation. This loss of nitrogen at this temperature is nearly five times larger than that due to the decrease of ammonia, inferred from the drop of the infrared absorption band at the top of Fig. 3. As seen for other gases [e.g., Ref. 25] this broad N<sub>2</sub> peak occurs during crystallization of the water ice that remains in the sample, possibly as a result of the enhanced diffusion paths along the newly formed grain boundaries. At higher temperatures, the small drop of the NH<sub>3</sub> absorption band and the increase of the NH signal in the MS due to NH<sub>3</sub> cracking indicate desorption of the ammonia that remained trapped in the ice after crystallization.

The peak in the desorption of water, seen between 115 and 130 K, was unexpected, because in both pure water ice (10) and in an unirradiated mixture, this degree of sublimation is only seen at much high temperatures. This desorption peak is not directly related to H<sub>2</sub> accumulation in the ice, since the fluence [ $1.2 \times 10^{15} \text{ ions}/\text{cm}^2$ ] that maximizes trapped H<sub>2</sub> [Fig. 1] is much smaller than that for maximum water desorption [ $7.5 \times 10^{15} \text{ ions}/\text{cm}^2$ ]. Since the water desorption peak is always accompanied by outbursts of H<sub>2</sub> and N<sub>2</sub>, we propose that these gases aggregate as high-pressure gas bubbles in radiation-induced voids in the ice (24). Once the pressure exceeds the fracture strength of ice, gas close to the surface will burst carrying some water with it. This mechanism seems to be directly related to the formation of spots we observe when the irradiated ice is warmed (Fig. 4). Such newly formed spots ( $\sim 5 \mu\text{m}$ ) act as scattering centers causing a decrease in the reflectance of the sample, as shown in Fig. 5.

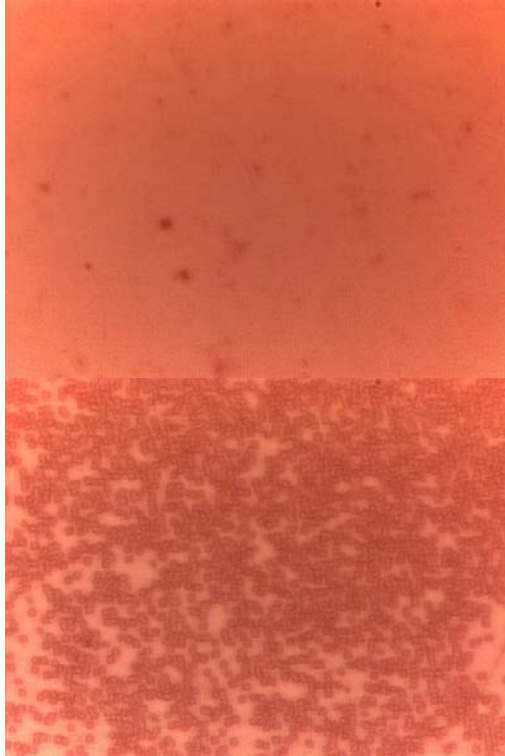


Figure 4. Warming of a 1:2 ammonia-water mixture irradiated with  $3 \times 10^{15} \text{ H}^+$  ions/cm<sup>2</sup>. Top: 70 K, Bottom: 117.42 K. The width of the picture is ~250 microns and height ~180 microns. We note that in this experiment the bursts peaked at 120 K.

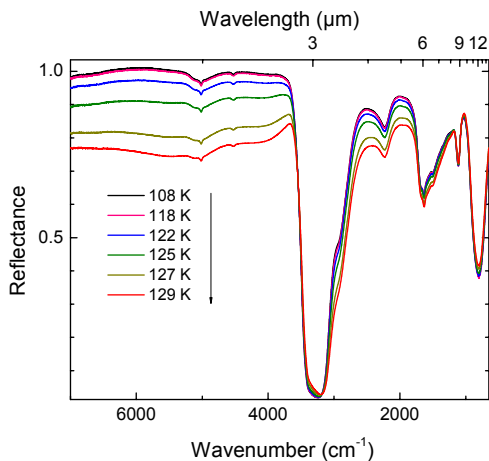


Figure 5. Evolution of the infrared reflectance of a 1:2 ammonia-water sample irradiated to  $7.5 \times 10^{15} \text{ H}^+$ /cm<sup>2</sup> at 70 K during warming at 0.2 K/min.

At Enceladus, a layer of ammonia dihydrate that resurfaces by some endogenic process will be irradiated by magnetospheric protons to a fluence of  $1 \times 10^{16} \text{ ions/cm}^2$  [or  $1 \times 10^{18} \text{ keV/cm}^2$ ] in ~25 years, using data from Jurac et al. (27). This time is probably a lower limit since the flux may be an overestimate (28), yet it is still many orders of magnitude lower than current estimates for the youngest terrain on Enceladus (12, 29). Magnetospheric ion irradiation will deplete the surface of ammonia, lowering the likelihood of detection by infrared reflectance (17) and eject hydrogen and nitrogen from the surface. The nitrogen emission provides an explanation for a source of nitrogen at Enceladus detected by the Cassini CAPS instrument (4, 5) and in the plume of Enceladus. The desorption of water at temperatures as low as 115 K may also help explain the water emission from the south polar region of Enceladus observed by Cassini's UVIS spectrometer (8). However before we can conclude whether our bursts during warming can adequately account for the spectacular plume observed, the time variance in the emission from the South Pole of Enceladus needs to be studied.

## References

1. A. J. Verbiscer, R. G. French, C. A. McGhee, *Icarus* **173**, 66 (2005).
2. B. A. Smith *et al.*, *Science* **215**, 505 (1982).
3. D. E. Shemansky, P. Matheson, D. T. Hall, H.-Y. Hu, T. M. Tripp, *Nature* **363**, 329 (1993).
4. H. T. Smith *et al.*, *Geophys. Res. Lett.* **32**, L14S03 (2005).
5. D. T. Young *et al.*, *Science* **307**, 1262 (2005).
6. J. R. Spencer *et al.*, *Science*, in press.
7. D. P. Cruikshank *et al.*, *Icarus* **175**, 268 (2005).
8. C. J. Hansen *et al.*, *Science*, in press.
9. C. C. Porco *et al.*, *Science*, in press.
10. N. J. Sack, R. A. Baragiola, *Phys. Rev. B* **48**, 9973 (1993).
11. S. W. Squyres, R. T. Reynolds, P. M. Cassen, *Icarus* **53**, 319 (1983).
12. J. S. Kargel, S. Pozio, *Icarus* **119**, 385 (1996).
13. J. Wisdom, *Astron. J.* **128**, 484 (2004).
14. D. J. Stevenson, *Nature* **298**, 142 (1982).
15. J. S. Lewis, *Icarus* **15**, 174 (1971).
16. L. J. Lanzerotti, W. L. Brown, K. J. Marcantonio, R. E. Johnson, *Nature* **312**, 139 (1984).
17. J. P. Emery, D. M. Burr, D. P. Cruikshank, R. H. Brown, J. B. Dalton, *Astron. Astrophys.* **435**, 353 (2005).
18. R. W. Carlson *et al.*, *Science* **283**, 2062 (1999).

19. K. S. Noll, T. L. Roush, D. P. Cruikshank, R. E. Johnson, Y. J. Pendleton, *Nature* **388**, 45 (1997).
20. S. M. Krimigis *et al.*, *J. Geophys. Res.* **88**, 8871 (1983).
21. J. F. Ziegler, *Stopping and Range of Ions in Matter SRIM2003* (available at [www.srim.org](http://www.srim.org)) (2003).
22. D. L. Hogenboom *et al.*, *Icarus* **128**, 171 (1997).
23. M. J. Loeffler, B. D. Teolis, R. A. Baragiola, *J. Chem. Phys.*, in press.
24. M. J. Loeffler, B. D. Teolis, R. A. Baragiola, *ApJ*, in press.
25. R. A. Vidal, D. Bahr, R. A. Baragiola, M. Peters, *Science* **276**, 1839 (1997).
26. D. Laufer, E. Kochavi, A. Bar-Nun, *Phys. Rev. B* **36**, 9219 (1987).
27. S. Jurac, R. E. Johnson, J. D. Richardson, C. Paranicas, *Planet. Science Sci.* **49**, 319 (2001).
28. C. Paranicas *et al.*, *Geophys. Res. Lett.* **31** (2004).
29. B. A. Smith *et al.*, *Science* **212**, 163 (1981).